







Research Article

Systematically Characterizing Chemical Profile and Potential Mechanisms of Qingre Lidan Decoction Acting on Cholelithiasis by Integrating UHPLC-QTOF-MS and Network Target Analysis

Peng Huang ^{1,2}, Hongwen Ke ³, Yang Qiu ⁴, Mingchen Cai ³,
Jialin Qu ¹ and Aijing Leng ^{2,3}

¹Clinical Laboratory of Integrative Medicine, The First Affiliated Hospital of Dalian Medical University, No. 222, Zhongshan Road, Dalian 116011, China

²Institute of Integrative Medicine, Dalian Medical University, No. 9, South Road of Lvshun, Dalian 116044, China

³Department of Traditional Chinese Medicine, The First Affiliated Hospital of Dalian Medical University, No. 222, Zhongshan Road, Dalian 116011, China

⁴Central Laboratory, The First Affiliated Hospital of Dalian Medical University, No. 222, Zhongshan Road, Dalian 116011, China

Correspondence should be addressed to Jialin Qu; jialin_qu@126.com and Aijing Leng; l18098877517@163.com

Received 2 August 2018; Revised 8 November 2018; Accepted 12 November 2018; Published 3 January 2019

Academic Editor: Armando Zarrelli

Copyright © 2019 Peng Huang et al. This is an open access article distributed under the Creative Commons Attribution License, which permits unrestricted use, distribution, and reproduction in any medium, provided the original work is properly cited.

Qingre Lidan Decoction (QRLDD), a classic precompounded prescription, is widely used as an effective treatment for cholelithiasis clinically. However, its chemical profile and mechanism have not been characterized and elucidated. In the present study, a rapid, sensitive, and reliable ultraperformance liquid chromatography coupled with quadrupole time-of-flight mass spectrometry method was established for comprehensively identifying the major constituents in QRLDD. Furthermore, a network pharmacology strategy based on the chemical profile was applied to clarify the synergetic mechanism. A total of 72 compounds containing flavonoids, terpenes, phenolic acid, anthraquinones, phenethylalcohol glycosides, and other miscellaneous compounds were identified, respectively. 410 disease genes, 432 compound targets, and 71 related pathways based on cholelithiasis-related and compound-related targets databases as well as related pathways predicted by the Kyoto Encyclopedia of Genes and Genomes database were achieved. Among these pathways and genes, pathway in cancer and MAPK signaling pathway may play an important role in the development of cholelithiasis. EGFR may be a crucial target in the conversion of gallstones to gallbladder carcinoma. Regulation of PRKCB/RAF1/MAP2K1/MAPK1 is associated with cell proliferation and differentiation. Thus, the fingerprint coupled with network pharmacology analysis could contribute to simplifying the complex system and providing directions for further research of QRLDD.

1. Introduction

Traditional Chinese Medicine possess a history of thousands of years, which has been widely used in clinical practice in China and played an increasingly important role to health maintenance and disease treatment. Traditional Chinese Formula (TCF) is the main form of clinical application of Traditional Chinese Medicine. Due to its satisfactory clinical efficacy, TCF has been regarded as an alternative and promising medicine strategy for treating complex diseases all over the world [1]. Qingre Lidan Decoction (QRLDD) is a classic precompounded prescription, which contains 6

herbs, namely, *Lysimachiae Herba* (jin-qian-cao in Chinese), *Scutellariae Radix* (huang-qin in Chinese), *Aurantii Fructus* (zhi-qiao in Chinese), *Aucklandiae Radix* (mu-xiang in Chinese), *Gardeniae Fructus* (zhi-zi in Chinese), and *Rhei Radix et Rhizoma* (da-huang in Chinese). It has been extensively applied in clinical treatment of cholecystitis and gallstones for many years with the satisfactory therapeutic effects in several hospitals [2, 3]. The main mechanism of its efficacy has been reported to relax sphincter of Oddi, promote bile excretion, and prevent stagnation [4]. However, the current research on QRLDD has two drawbacks: firstly, a clear understanding of the relationship between ingredient and formula has

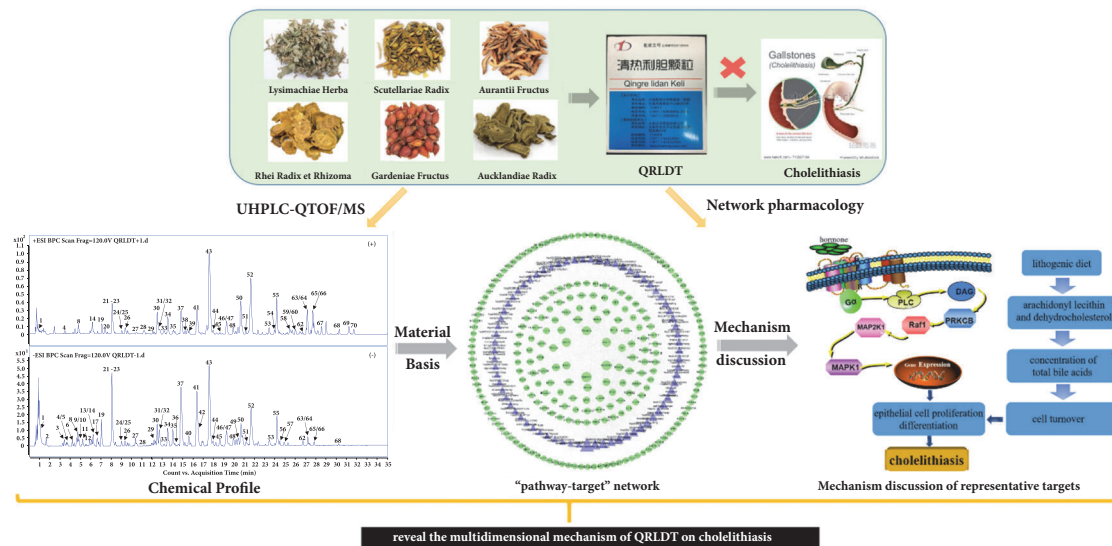


FIGURE 1: Schematic diagram of present study.

not been elucidated; secondly, in aspect of pharmaceutical effect, current reports usually focus on the level of single inflammatory mediator or protein, which is hardly to reflect the characteristic of multicomponents and multitargets of Chinese medicine formula [5]. These are obstacles for the development and the therapeutic efficacy of QRLDD.

In recent years, the rapid development of network pharmacology has provided a novel method for revealing the molecular mechanisms associated with the therapeutic efficacy of multicomponent in TCF [6]. It has facilitated understanding the interactions of ingredient, target, and disease systematically based on systems biology, polypharmacology, and molecular network analysis, rather than an individual target [7]. Thus, the application of network pharmacology provides a powerful and promising method for analyzing TCF.

The schematic diagram of present study was shown in Figure 1; an ultraperformance liquid chromatography coupled with quadrupole time-of-flight mass spectrometry (UHPLC-QTOF-MS) method was established to analyze the major chemical constituents of QRLDD in this present study. Potential targets and related pathways were correspondingly explored by using network pharmacology method based on the identified components, and the mechanism of QRLDD in the treatment of cholelithiasis was elucidated systematically.

2. Materials and Methods

2.1. Chemicals, Reagents, and Materials. UHPLC-MS grade acetonitrile and methanol were purchased from Merck Company Inc. (Darmstadt, Germany) and MS grade formic acid was supplied by Fisher Scientific Company Inc. (Fairlawn, NJ). Ultrapure water (18.2 M Ω) was prepared with a Milli-Q water purification system (Millipore, Milford, MA, USA). All other reagents were of analytical grade and purchased from Tianjin Concord Technology Co. Ltd. (Tianjin, China)

The reference compounds gallic acid (2), protocatechuic acid (3), 4-hydroxybenzoic acid (10), (+) catechin (13), chlorogenic acid (15), caffeic acid (17), syringing (20), geniposide (21), (-)-epicatechin (22), rutin (29), kaempferol (36), hesperidin (40), neohesperidin (41), baicalin (43), quercetin (47), baicalein (55), aloe-emodin (60), rhein (61), wogonin (64), emodin (68), dehydrocostuslactone (70), chrysophanol (71), and physcion (72) were purchased from the National Institutes for Food and Drug Control (Beijing, China). The purity of each reference standard was determined to be over 98% by UHPLC analysis. All the 6 herbs of QRLDD, including Lysimachiae Herba, Scutellariae Radix, Aurantii Fructus, Aucklandiae Radix, Gardeniae Fructus, and Rhei Radix et Rhizoma, were purchased from the first affiliated hospital of Dalian Medical University (Dalian, Liaoning Province, China), and authenticated by Professor Aijing Leng (Department of Chinese medicine, The First Affiliated Hospital of Dalian Medical University). Voucher specimens were deposited at the authors' laboratory.

2.2. Preparation of Samples and Standard Solution. The QRLDD samples were prepared by the decocting method. A blended mixture of Lysimachiae Herba (30 g), Scutellariae Radix (15 g), Aucklandiae Radix (15 g), Aurantii Fructus (15 g), and Gardeniae Fructus (15 g) was soaked in 10-fold mass of water (900 mL) for 1 h and boiled for 1 h and then filtered with six-layer absorbent gauze. An 8-fold mass of water (800 mL) was subsequently added to residues and boiled for 30 min. Then Rhei Radix et Rhizoma (10 g) was added into the extract and boiled for additional 30 min. After being filtered with six-layer absorbent gauze, the two filtrates were combined and concentrated under vacuum to 100 mL (equal to 1 g crude herb/mL), and finally the concentrate was transformed into the freeze-dried powder.

A 1.0 g of the freeze-dried powder was accurately weighted and extracted with 50 mL of methanol/water (1:1, v/v) for 30 min under ultrasound. The extract solution

was centrifuged at 13000 rpm for 10 min at 4°C, and the supernatant was filtered through a 0.22 µm filter. 1.0 µL of filtrate was injected to UHPLC-QTOF-MS for analysis.

2.3. Chromatography and MS Conditions. Chromatographic separation was performed on an Agilent 1290 Infinity LC system (Agilent, USA) using an Agilent Zorbax Eclipse Plus C18 column (100 × 2.1 mm i.d., 3.5 µm). The oven temperature was maintained at 40°C. Water containing 0.1% formic acid (solvent system A) and acetonitrile (solvent system B) served as the mobile phase. The gradient elution program was 0–5 min, 3%–10% B; 5–13 min, 10%–18% B; 13–20 min, 18%–25% B; 20–28 min, 25%–35% B; 28 to 33 min, 35% to 99% B; 33–35 min, 99%–3% B; 35–40 min, 3% B.

Mass detection was performed using an Agilent 6530B Accurate-Mass Quadrupole Time-of-Flight (Q-TOF) mass spectrometer (Agilent Corp., USA) equipped with a Dual AJS ESI source operating in both positive and negative mode with the following operating parameters: drying gas (N₂) flow rate, 10.0 L/min; drying gas (N₂) temperature, 350°C; nebulizer, 35 psig; sheath gas (N₂) temperature, 400°C; fragmentor voltage, 120 V; skimmer voltage, 65 V; Octopole RF, 750 V. The capillary voltage was set at 4 kV or –3.5 kV under positive or negative mode, respectively. The nozzle voltage was set at +500 V or –1000 V, respectively; four collision energies at 10 V, 20 V, 30 V, and 40 V were applied to acquire sufficient product ions. MS spectra were recorded over the m/z range of 50–1100. All data was processed by MassHunter workstation software version B.06.00 (Agilent Technologies, Germany).

2.4. Target Network Pharmacology Analysis

2.4.1. Therapeutic Targets of Cholelithiasis. Cholelithiasis associated targets were obtained from six existing resources: (1) TTD database (<http://bidd.nus.edu.sg/BIDD-Databases/TTD/TTD.asp>), which could provide a comprehensive information platform about the clinical trial drugs, targets and pathways [8]; (2) OMIM database (<http://omim.org/>), which catalogues all known diseases with a genetic component and provides references for further research and tools for genomic analysis of a catalogued gene [9]; (3) PharmGKB database (<https://www.pharmgkb.org/>), which provides a various array of PGx information, from annotations of the primary literature to guidelines for adjusting drug treatment based on genetic information [10]; (4) DrugBank database (<http://www.drugbank.ca/>, version 4.3), which includes >4100 drug entries, >14 000 protein or drug target sequences that relevant to these drug entries [11]; (5) GAD database (<https://geneticassociationdb.nih.gov/>), which provides a platform analysis for complex common human genetic disease systematically [12]. (6) DisGeNET database (<http://www.disgenet.org/web/DisGeNET/menu>), which offers available collections of genes and variants related to human diseases [13].

We searched these databases with keywords “cholecystitis”, “acute cholecystitis”, “chronic cholecystitis”, “gallstones”, “cholangitis”, “jaundice”, “obstructive jaundice” and got 410 genes totally after removing duplicates. The detailed information is provided in Supplementary Table S1.

2.4.2. Compound Target for QRLDD. After identifying the compounds contained in QRLDD by UHPLC-QTOF-MS/MS, the InChI Key, Canonical SMILES, and CAS number of compounds were obtained from NCBI PubChem database (<https://www.ncbi.nlm.nih.gov/pubmed/>). And ingredient-related targets were accordingly collected from the Traditional Chinese Medicine Systems Pharmacology Database and Analysis Platform (TCMSP) (<http://lsp.nwu.edu.cn/tcmsp.php>) and Swiss Target Prediction (<http://www.swisstargetprediction.ch/>) with their names and/or CAS number as key words. Then, their official symbol was obtained after input of the targets with the species limited to “Homo sapiens” via UniProtKB (<http://www.uniprot.org/>) [14]. Finally, genes information of ingredients was achieved. The details are supplied in Supplementary Table S2.

2.4.3. The Protein–Protein Interactions (PPIs) Network Analysis. The protein–protein interactions (PPIs) network was constructed and analyzed by STRING database. In order to further identify the primary therapeutic targets to guarantee the accuracy of results, only those PPIs with high confidence score (>0.95) were selected for network construction and analysis [15].

2.4.4. Network Construction and Analysis. All the networks can be performed by utilizing the network visualization software Cytoscape 3.2.1 [16], which supplies a method for data integration, analysis, and visualization for complicated network analysis. Three networks were constructed as follows: (1) protein-protein interactions (PPIs) of cholelithiasis targets; (2) herb-compound-compound targets network of QRLDD; (3) pathways-targets network analysis. In this network plot, a “node” signifies an herb, ingredient, or gene; an “edge” represents interaction among different targets. The “degree” of a node was in agreement with the number of its connected edges [17].

2.4.5. Enrichment Analysis. To clarify the pathways that are relate to putative QRLDD targets, Kyoto Encyclopedia of Genes and Genomes (KEGG) pathway enrichments based on Database for Annotation, Visualization and Integrated Discovery (DAVID, <https://david.ncifcrf.gov/home.jsp>, ver. 6.8) were applied [18].

3. Results and Discussion

3.1. Chemical Profile of QRLDD by UHPLC-QTOF-MS. In the present study, a specific UHPLC-ESI-QTOF MSⁿ protocol was performed to rapidly identify the compounds of QRLDD based on the optimized LC and MS conditions systematically.

As a result, a total of 72 compounds, including 33 flavonoids, 17 terpene, 9 phenolic acid, 5 anthraquinones, 3 phenethylalcohol glycosides, and 5 miscellaneous compounds were identified or tentatively characterized (Figure 2, Table 1). Among them, 23 constituents (compounds 2-3, 10, 13, 15, 17, 20-22, 29, 36, 40-41, 43, 47, 55, 60-61, 64, 68, and 70-72) were unambiguously identified as gallic acid, protocatechuic acid, 4-hydroxybenzoic acid, (+)-catechin,

TABLE 1: Characterization of the chemical constituents in QRLDD by UHPLC-QTOF-MS.

Peak No	t_R (min)	Identification	Formula	Negative ion			Positive ion			Source ^a				
				Quasi-molecular ion	Observed mass (Da)	Calculated mass (Da)	ppm	Fragment ions	Quasi-molecular ion		Observed mass (Da)	Calculated mass (Da)	ppm	Fragment ions
1	1.54	Galloyl glucose	$C_{13}H_{16}O_{10}$	$[M-H]^-$	331.0678	331.0671	2.11	287[M-H-CO ₂] 169[M-H-C ₆ H ₁₀ O ₅] 125[M-H-C ₆ H ₁₀ O ₅ -CO ₂]	$[M+Na]^+$	355.0644	355.0636	2.25	311[M+Na-CO ₂] ⁺ 338[M+Na-OH] ⁺ 193[M+Na-C ₆ H ₁₀ O ₅] ⁺ 153[M+H-H ₂ O] ⁺ 127[M+H-CO ₂] ⁺	RRR
2 ^b	1.69	Gallic acid	$C_7H_6O_5$	$[M-H]^-$	169.0147	169.0142	2.96	151[M-H-H ₂ O] 108[M-H-CHO ₂] 125[M-H-CO ₂]	$[M+H]^+$	171.0289	171.0288	0.58	153[M+H-H ₂ O] ⁺ 127[M+H-CO ₂] ⁺	EA
3 ^b	3.32	Protocatechuic acid	$C_7H_6O_4$	$[M-H]^-$	153.0200	153.0193	4.57	109[M-H-CO ₂] 361[M-H-CO ₂] 317[M-H-2CO ₂]	—	—	—	—	—	SR/EA
4	3.58	Shanzhiside methyl ester	$C_{17}H_{26}O_{11}$	$[M-H]^-$	405.1400	405.1402	-0.49	225[M-H-gal-H ₂ O] 229[M-H-C ₆ H ₁₀ O ₅] 185[M-H-C ₆ H ₁₀ O ₅ -CO ₂] 167[M-H-C ₆ H ₁₀ O ₅ -H ₂ O-CO ₂]	$[M+Na]^+$	429.1387	429.1367	4.66	—	GF
5	3.68	Shanzhiside	$C_{16}H_{24}O_{11}$	$[M-H]^-$	391.1243	391.1246	-0.77	—	—	—	—	—	—	GF
6	4.26	Gardenoside	$C_{17}H_{24}O_{11}$	$[M+HCOO]^-$	449.1308	449.1301	1.56	403.289[M-H-C ₂ H ₁₀ O ₅]	$[M+Na]^+$	427.1176	427.1211	-8.19	—	GF
7	4.44	Neochlorogenic acid	$C_{17}H_{24}O_{11}$	$[M-H]^-$	403.1265	403.1246	4.71	—	—	—	—	—	—	GF
8	4.65	Jasminoside D	$C_{16}H_{26}O_8$	$[M-H]^-$	353.0882	353.0878	1.13	191[M-H-C ₉ H ₆ O ₃]	$[M+H]^+$	347.1683	347.1700	-4.90	311[M+H-2H ₂ O] ⁺	GF
9	4.72	Scandoside methyl ester	$C_{17}H_{24}O_{11}$	$[M+HCOO]^-$	449.1300	449.1301	-0.22	241[M-H-C ₆ H ₁₀ O ₅]	$[M+Na]^+$	427.1186	427.1211	-5.85	—	GF
10 ^b	4.80	4-Hydroxybenzoic acid	$C_7H_6O_3$	$[M-H]^-$	403.1271	403.1246	6.20	93[M-H-CO ₂]	$[M+H]^+$	139.0383	139.0390	-5.03	—	SR/EA
11	5.40	Procyanidin B2	$C_{30}H_{26}O_{12}$	$[M-H]^-$	137.0246	137.0244	1.46	559[M-H-H ₂ O] 535[M-H-C ₂ H ₂ O]	$[M+H]^+$	579.1469	579.1497	-4.83	—	RRR
12	5.93	Jasminoside B	$C_{16}H_{26}O_8$	$[M+HCOO]^-$	577.1351	577.1351	0.00	183[M-H-C ₆ H ₁₀ O ₅] 165[M-H-C ₆ H ₁₀ O ₅ -H ₂ O] 121[M-H-C ₆ H ₁₀ O ₅ -CO ₂] 245[M-H-CO ₂]	—	—	—	—	—	GF
13 ^b	6.16	(+)-Catechin	$C_{15}H_{14}O_6$	$[M+Cl]^-$	289.0727	289.0718	3.11	247[M-H-C ₂ H ₂ O] 179[M-H-C ₆ H ₆ O ₂] 271[M-H-H ₂ O]	$[M+H]^+$	291.0841	291.0863	-7.56	—	AF/RRR

TABLE I: Continued.

Peak No	t_R (min)	Identification	Formula	Negative ion				Positive ion				Source ^a		
				Quasi-molecular ion	Observed mass (Da)	Calculated mass (Da)	ppm	Fragment ions	Quasi-molecular ion	Observed mass (Da)	Calculated mass (Da)		ppm	
14	6.23	Gardenone	$C_{12}H_{20}O_3$	$[M+HCOO]^-$	257.1393	257.1394	-0.39	213[M-H-CO ₂]	—	—	—	—	GF	
15 ^b	6.30	Chlorogenic acid	$C_{16}H_{18}O_9$	$[M-H]^-$ $[2M-H]^-$	353.0890 707.1834	353.0878 707.1829	3.40 0.71	191[M-H-C ₉ H ₆ O ₃] 179[M-H-C ₉ H ₁₀ O ₅] 135[M-H-C ₈ H ₁₀ O ₇]	$[M+H]^+$	355.1003	355.1024	-5.91	—	GF
16	6.46	Darendoside A	$C_{19}H_{28}O_{11}$	$[M-H]^-$	431.1561	431.1559	0.46	—	—	—	—	—	—	SR
17 ^b	6.74	Caffeic acid	$C_9H_8O_4$	$[M-H]^-$	179.0357	179.0350	3.91	135[M-H-CO ₂]	$[M+H]^+$	181.0483	181.0495	-6.63	—	SR/EA
18	6.85	Cryptochlorogenic acid	$C_{16}H_{18}O_9$	$[M-H]^-$	353.0883	353.0878	1.42	179[M-H-C ₉ H ₁₀ O ₅]	—	—	—	—	—	GF
19	7.11	Genipin-1- β -gentiobioside	$C_{23}H_{34}O_{15}$	$[M-H]^-$	549.1830	549.1825	0.91	225[M-H-2C ₆ H ₁₀ O ₅]	$[M+Na]^+$	573.1794	573.1790	0.70	—	GF
20 ^b	7.60	Syringin	$C_{17}H_{24}O_9$	$[M+HCOO]^-$	595.1879	595.1880	-0.17	207[M-H-2C ₆ H ₁₀ O ₅ -H ₂ O]	—	—	—	—	—	GF
21 ^b	8.11	Geniposide	$C_{17}H_{24}O_{10}$	$[M+HCOO]^-$	417.1401	417.1402	-0.24	373[M-H-CO ₂]	$[M+Na]^+$	395.1300	395.1313	-3.29	—	RA
				$[M-H]^-$	387.1308	387.1297	2.84	225[M-H-C ₆ H ₁₀ O ₅]	$[M+Na]^+$	411.1286	411.1262	5.84	—	GF
				$[M+HCOO]^-$	433.1351	433.1352	-0.23	207[M-H-C ₆ H ₁₀ O ₅ -H ₂ O] 123[M-H-C ₁₀ H ₁₆ O ₈] 101[M-H-C ₁₃ H ₁₈ O ₇]	—	—	—	—	—	—
22 ^b	8.16	(-)-Epicatechin	$C_{15}H_{14}O_6$	$[M-H]^-$	289.0721	289.0718	1.04	245[M-H-CO ₂]	$[M+H]^+$	291.0868	291.0863	1.72	—	AF
				$[M+Cl]^-$	325.0488	325.0484	1.23	179[M-H-C ₆ H ₆ O ₂]	—	—	—	—	—	—
23	8.17	Genipin	$C_{11}H_{14}O_5$	$[M-H]^-$	225.0772	225.0768	1.78	207[M-H-H ₂ O]	$[M+H]^+$	227.0917	227.0914	1.32	209[M+H-H ₂ O] ⁺	GF
				$[M-H]^-$	163.0406	163.0401	3.07	163[M-H-H ₂ O-CO ₂]	—	—	—	—	—	—
24	9.05	p-Coumaric acid	$C_9H_8O_3$	$[M-H]^-$	163.0406	163.0401	3.07	119[M-H-CO ₂]	$[M+H]^+$	165.0547	165.0546	0.61	147[M+H-H ₂ O] ⁺	SR
25	9.06	Nicotiflorin	$C_{27}H_{30}O_{15}$	$[M-H]^-$	593.1518	593.1512	1.01	285[M-H-rha-glu]	$[M+H]^+$	595.1657	595.1657	0.00	—	GF
				$[M-H]^-$	407.1010	407.0984	6.39	151[M-H-C ₁₉ H ₂₂ O ₁₂]	$[M+H]^+$	409.1119	409.1129	-2.44	—	AF

TABLE I: Continued.

Peak No	t_R (min)	Identification	Formula	Negative ion				Positive ion				Source ^a		
				Quasi-molecular ion	Observed mass (Da)	Calculated mass (Da)	ppm	Fragment ions	Quasi-molecular ion	Observed mass (Da)	Calculated mass (Da)		ppm	Fragment ions
27	10.58	Schaftoside/Isoschaftoside	$C_{26}H_{28}O_{14}$	$[M-H]^-$	563.1407	563.1406	0.18	503[M-H-C ₂ H ₄ O ₂], 443[M-H-2C ₂ H ₄ O ₂]	$[M+H]^+$	565.1544	565.1552	-1.42	547[M+H-H ₂ O] ⁺ 529[M+H-CO ₂] ⁺	SR/EA
28	11.25	Rhoifolin	$C_{27}H_{30}O_{14}$	$[M-H]^-$	577.1562	577.1563	-0.17		$[M+H]^+$	579.1700	579.1708	-1.38		AF
29 ^b	12.21	Rutin	$C_{27}H_{30}O_{16}$	$[M-H]^-$	609.1466	609.1461	0.82	301[M-H-rha-gla]	$[M+H]^+$	611.1593	611.1607	-2.29	303[M+H-rha-glc] ⁺	GF/EA
30	12.60	Scutellarin	$C_{21}H_{18}O_{12}$	$[M-H]^-$	461.0724	461.0725	-0.22	151[M-H-C ₂₀ H ₂₇ O ₁₂] 178[M-H-C ₁₉ H ₂₇ O ₁₁]	$[M+Na]^+$	633.1425	633.1426	-0.16		
31	12.74	Carthamidin	$C_{15}H_{12}O_6$	$[M-H]^-$	—	—	—	285[M-H-glc]	$[M+H]^+$	463.0877	463.0871	1.30		SR
32	12.78	Neorocitrin	$C_{27}H_{32}O_{15}$	$[M-H]^-$	595.1671	595.1668	0.50		$[M+H]^+$	289.0693	289.0707	-4.84		SR
33	13.13	Isoquercitrin	$C_{21}H_{20}O_{12}$	$[M-H]^-$	463.0880	463.0882	-0.43	301[M-H-C ₆ H ₁₀ O ₅] 300[M-H-C ₆ H ₁₁ O ₅]	$[M+H]^+$	597.1824	597.1814	1.67		AF
34	13.66	Acteoside	$C_{29}H_{36}O_{15}$	$[M-H]^-$	623.1969	623.1981	-1.93	461[M-H-C ₆ H ₁₀ O ₅] 315[M-H-rha]	$[M+Na]^+$	647.1916	647.1946	-4.64		SR
35	14.09	Narirutin	$C_{27}H_{32}O_{14}$	$[M-H]^-$	579.1709	579.1719	-1.73	271[M-H-rha-gla]	$[M+H]^+$	581.1852	581.1865	-2.24		AF
36	14.36	Kaempferol	$C_{15}H_{10}O_6$	$[M+Cl]^-$	615.1490	615.1486	0.65		$[M+Na]^+$	603.1682	603.1684	-0.33		
37	14.86	Naringin	$C_{27}H_{32}O_{14}$	$[M-H]^-$	285.0410	285.0405	1.75	241[M-H-CO ₂]	$[M+H]^+$	287.0544	287.0550	-2.09	153[M+H-C ₈ H ₆ O ₂] ⁺ 435[M+H-C ₆ H ₁₀ O ₄] ⁺	EA
				$[M+Cl]^-$	579.1728	579.1719	1.55	271[M-H-rha-gla]	$[M+H]^+$	581.1847	581.1865	-3.10	273[M+H-rha-gla] ⁺	AF
					615.1482	615.1486	-0.65	151[M-H-C ₂₀ H ₂₈ O ₁₀] 119[M-H-C ₁₉ H ₂₄ O ₁₃] 107[M-H-C ₂₀ H ₂₈ O ₁₀ -CO ₂] 259[M-H-rha-gla-C ₃ O ₂] 203[M-H-rha-gla-C ₃ O ₂ -C ₂ H ₂ O]	$[M+Na]^+$	603.1672	603.1684	-1.99		

TABLE I: Continued.

Peak No	t_R (min)	Identification	Formula	Negative ion				Positive ion				Source ^a		
				Quasi-molecular ion	Observed mass (Da)	Calculated mass (Da)	ppm	Fragment ions	Quasi-molecular ion	Observed mass (Da)	Calculated mass (Da)		ppm	Fragment ions
38	15.25	Isorhoifolin	$C_{27}H_{30}O_{14}$	$[M-H]^-$	577.1566	577.1563	0.52		$[M+H]^+$	579.1701	579.1708	-1.21		AF
39	15.37	Jasminoside S/H/I	$C_{22}H_{36}O_{12}$	$[M+HCOO]^-$	537.2186	537.2189	-0.56	375[M-H-C ₆ H ₁₀ O ₅] 167[M-H-2C ₆ H ₁₀ O ₅]	$[M+Na]^+$	515.2085	515.2099	-2.72		GF
				$[M+Cl]^-$	527.1899	527.1901	-0.38		—	—	—	—		
				$[M-H]^-$	491.2123	491.2134	-2.24		—	—	—	—		
40 ^b	15.65	Hesperidin	$C_{28}H_{34}O_{15}$	$[M-H]^-$	609.1829	609.1825	0.66	301[M-H-gla-rha]	$[M+H]^+$	611.1954	611.1970	-2.62	449[M+H-gla] ⁺ 303[M+H-gla-rha] ⁺	AF
				$[M+Cl]^-$	645.1600	645.1592	1.24		$[M+Na]^+$	633.1781	633.1790	-1.42		
41 ^b	16.44	Neohesperidin	$C_{28}H_{34}O_{15}$	$[M-H]^-$	609.1823	609.1825	-0.33	463[M-H-rha]	$[M+H]^+$	611.1961	611.1970	-1.47	449[M+H-gla] ⁺	AF
				$[M+Cl]^-$	645.1587	645.1592	-0.78	301[M-H-gla-rha]	$[M+Na]^+$	633.1782	633.1790	-1.26	303[M+H-gla-rha] ⁺	
42	16.71	Viscidulin III	$C_{17}H_{14}O_8$	$[M-H]^-$	345.0626	345.0616	2.90	301[M-H-CO ₂]	$[M+H]^+$	347.0748	347.0761	-3.75		SR
43 ^b	17.60	Baicalin	$C_{21}H_{18}O_{11}$	$[M-H]^-$	445.0773	445.0776	-0.67	269[M-H-gluA]	$[M+Na]^+$	469.0731	469.0741	-2.13		SR
				$[2M-H]^-$	891.1628	891.1625	0.34	251[M-H-H ₂ O] 241[M-H-CO] 225[M-H-CO ₂]	$[M+H]^+$	447.0920	447.0922	-0.45		
								223[M-H-H ₂ O-CO] 207[M-H-H ₂ O-CO ₂]	—	—	—	—		GF
44	18.03	Crocin-1	$C_{44}H_{64}O_{24}$	$[M-H]^-$	975.3737	975.3715	2.26	651[M-H-2C ₆ H ₁₀ O ₅]	—	—	—	—		
				$[M+Cl]^-$	1011.3496	1011.3482	1.38	327[M-H-4C ₆ H ₁₀ O ₅]	—	—	—	—		
45	18.694	Dihydrobaicalin	$C_{21}H_{20}O_{11}$	$[M-H]^-$	447.0942	447.0933	2.01	411[M-H-2H ₂ O]	$[M+H]^+$	449.1069	449.1078	-2.00		SR
				$[2M-H]^-$	895.1931	895.2012	-9.05	271[M-H-gluA] 253[M-H-gluA-H ₂ O]	$[M+Na]^+$	471.0884	471.0898	-2.97		

TABLE I: Continued.

Peak No	t_R (min)	Identification	Formula	Negative ion				Positive ion				Source ^a		
				Quasi-molecular ion	Observed mass (Da)	Calculated mass (Da)	ppm	Fragment ions	Quasi-molecular ion	Observed mass (Da)	Calculated mass (Da)		ppm	Fragment ions
46	19.51	Cistanoside D	$C_{31}H_{40}O_{15}$	[M-H] ⁻	651.2281	651.2294	-2.00	475[M-H-gluA]	[M+Na] ⁺	675.2240	675.2259	-2.81	SR	
47 ^b	19.54	Quercetin	$C_{15}H_{10}O_7$	[M+Cl] ⁻	687.2063	687.2061	0.29	15[M-H-C ₆ H ₈ O ₃]	[M+H] ⁺	303.0492	303.0499	-2.31	285[M+H-H ₂ O] ⁺ 257[M+H-H ₂ O-CO] ⁺	GF/EA
48	20.13	Crocin-2	$C_{38}H_{54}O_{19}$	[M-H] ⁻	813.3186	813.3187	-0.12	65[M-H-C ₆ H ₁₀ O ₅] 489[M-H-2C ₆ H ₁₀ O ₅] 327[M-H-3C ₆ H ₁₀ O ₅] 283[M-H-gluA] 268[M-H-gluA-CH ₃]	[M+Na] ⁺	837.3156	837.3152	0.48	GF	
49	20.68	Wogonoside	$C_{22}H_{20}O_{11}$	[M-H] ⁻	459.0953	459.0933	4.36		[M+H] ⁺	461.1091	461.1078	2.82	443[M+H-H ₂ O] ⁺ 285[M+H-gluA] ⁺ 270[M+H-gluA-CH ₃] ⁺	SR
50	20.75	Cistanoside C	$C_{31}H_{40}O_{15}$	[M-H] ⁻	651.2295	651.2294	0.15	475[M-H-gluA]	[M+Na] ⁺	675.2255	675.2259	-0.59	SR	
51	21.26	Pectolinarin	$C_{29}H_{34}O_{15}$	[M+Cl] ⁻	687.2066	687.2061	0.73		[M+H] ⁺	623.1958	623.1970	-1.93	AF	
52	21.69	Baicalin O-gluA methylester	$C_{22}H_{20}O_{11}$	[M-H] ⁻	459.0949	459.0933	3.49		[M+H] ⁺	461.1086	461.1078	1.73	SR	
53	23.62	Hesperetin	$C_{16}H_{14}O_6$	[M-H] ⁻	301.0723	301.0718	1.66		[M+Na] ⁺	483.0886	483.0898	-2.48	AF	
54	23.99	Tenaxin II	$C_{16}H_{12}O_6$	[M-H] ⁻	299.0569	299.0561	2.68	284[M-H-CH ₃]	[M+H] ⁺	301.0701	301.0707	1.99	-286[M+H-CH ₃] ⁺	SR
55 ^b	24.20	Baicalin	$C_{15}H_{10}O_5$	[M-H] ⁻	269.0455	269.0455	0.00	251[M-H-H ₂ O] 241[M-H-CO] 181[M-H-CO-O-CO ₂] 225[M-H-CO-O] 223[M-H-H ₂ O-CO]	[M+H] ⁺	271.0579	271.0601	-8.12	GF	

TABLE I: Continued.

Peak No	t_R (min)	Identification	Formula	Negative ion				Positive ion				Source ^a		
				Quasi-molecular ion	Observed mass (Da)	Calculated mass (Da)	ppm	Fragment ions	Quasi-molecular ion	Observed mass (Da)	Calculated mass (Da)		ppm	Fragment ions
56	24.49	Crocin-4	$C_{44}H_{64}O_{24}$	$[M-H]^-$	975.3725	975.3715	1.03						GF	
57	24.89	Tenaxin II isomer	$C_{16}H_{12}O_6$	$[M-H]^-$	299.0558	299.0561	-1.00	284[M-H-CH ₃]	$[M+H]^+$	301.0697	301.0707	-3.32	286[M+H-CH ₃] ⁺	SR
58	25.72	Meranzin	$C_{15}H_{16}O_4$						$[M+Na]^+$	283.0940	283.0941	-0.35		AF
59	26.03	Dikamaliartanes A	$C_{30}H_{44}O_6$						$[M+Na]^+$	523.3043	523.3030	2.48	239[M+H-CO ₂] ⁺	GF
60 ^b	26.02	Aloe-emodin	$C_{15}H_{10}O_5$	$[M-H]^-$	269.0466	269.0455	4.09	239[M-H-CH ₂ O] 211[M-H-CO]	$[M+H]^+$	271.0589	271.0601	-4.43		RRR
61	26.71	Rhein	$C_{15}H_8O_6$	$[M-H]^-$	283.0256	283.0248	2.83	183[M-H-CO-CO] 255[M-H-CO] 239[M-H-CO ₂] 183[M-H-CO ₂ -2CO] 211[M-H-CO ₂ -CO] 183[M-H-CO-2CO]						RRR
62	26.76	Limomin	$C_{26}H_{30}O_8$	$[M-H]^-$	469.1875	469.1868	1.49		$[M+H]^+$	471.2006	471.2013	-1.49		AF
63	27.11	Skullcapflavone	$C_{18}H_{16}O_7$	$[M+Cl]^-$	505.1631	505.1635	-0.79							SR
64 ^b	27.20	Wogomin	$C_{16}H_{12}O_5$	$[M-H]^-$	283.0620	283.0612	2.83	240[M-H-CH ₃ -COH] 239[M-H-CH ₃ -COH] 223[M-H-CH ₃ -CO ₂ H] 212[M-H-CH ₃ -2CO]	$[M+H]^+$	285.0745	285.0757	-4.21		SR
65	27.86	Skullcapflavon II	$C_{19}H_{18}O_8$	$[M-H]^-$	373.0938	373.0929	2.41	358[M-H-CH ₃] 343[M-H-2CH ₃] 257[M-H-4CH ₃ -2CO] 328[M-H-3CH ₃] 300[M-H-3CH ₃ -CO] 272[M-H-3CH ₃ -2CO]	$[M+H]^+$	375.1073	375.1074	-0.27	345[M+H-2CH ₃] ⁺	SR

TABLE 1: Continued.

Peak No	t_R (min)	Identification	Formula	Negative ion				Positive ion				Source ^a	
				Quasi-molecular ion	Observed mass (Da)	Calculated mass (Da)	ppm	Fragment ions	Quasi-molecular ion	Observed mass (Da)	Calculated mass (Da)		ppm
66	27.87	Oroxylin A	$C_{16}H_{12}O_5$	$[M-H]^-$	283.0619	283.0612	2.47	268[M-H-CH ₃] 239[M-H-COH]	$[M+H]^+$	285.0754	285.0757	-1.05	SR
67	28.67	Tenaxin I	$C_{18}H_{16}O_7$	$[M-H]^-$	343.0831	343.0823	2.33	328[M-H-CH ₃] 313[M-H-2CH ₃] 298[M-H-3CH ₃]	$[M+H]^+$	345.0963	345.0969	-1.74	SR
68 ^b	30.24	Emodin	$C_{15}H_{10}O_5$	$[M-H]^-$	269.0453	269.0455	-0.74	251[M-H-H ₂ O] 241[M-H-CO] 225[M-H-CO-O] 181[M-H-CO-O-CO ₂]	$[M+H]^+$	271.0600	271.0601	-0.37	RRR/EA
69	31.27	Costunolide	$C_{15}H_{20}O_2$	—	—	—	—	—	$[M+H]^+$	233.1535	233.1536	-0.43	RA
70 ^b	31.80	Dehydrocostuslactone	$C_{15}H_{18}O_2$	—	—	—	—	—	$[M+H]^+$	231.1357	231.1380	-9.95	RA
71 ^b	32.99	Chrysophanol	$C_{15}H_{10}O_4$	—	—	—	—	—	$[M+H]^+$	255.0638	255.0652	-5.49	RRR
72 ^b	34.51	Physcion	$C_{16}H_{12}O_5$	—	—	—	—	—	$[M+H]^+$	285.0765	285.0757	2.81	RRR

^a RRR, Rhei Radix et Rhizoma; EA, Lysimachiae Herba; SR, Scutellariae Radix; GF, Gardeniae Fructus; AR, Aucklandiae Radix; AF, Aurantii Fructus.

^b Components identified with reference compounds comparison.

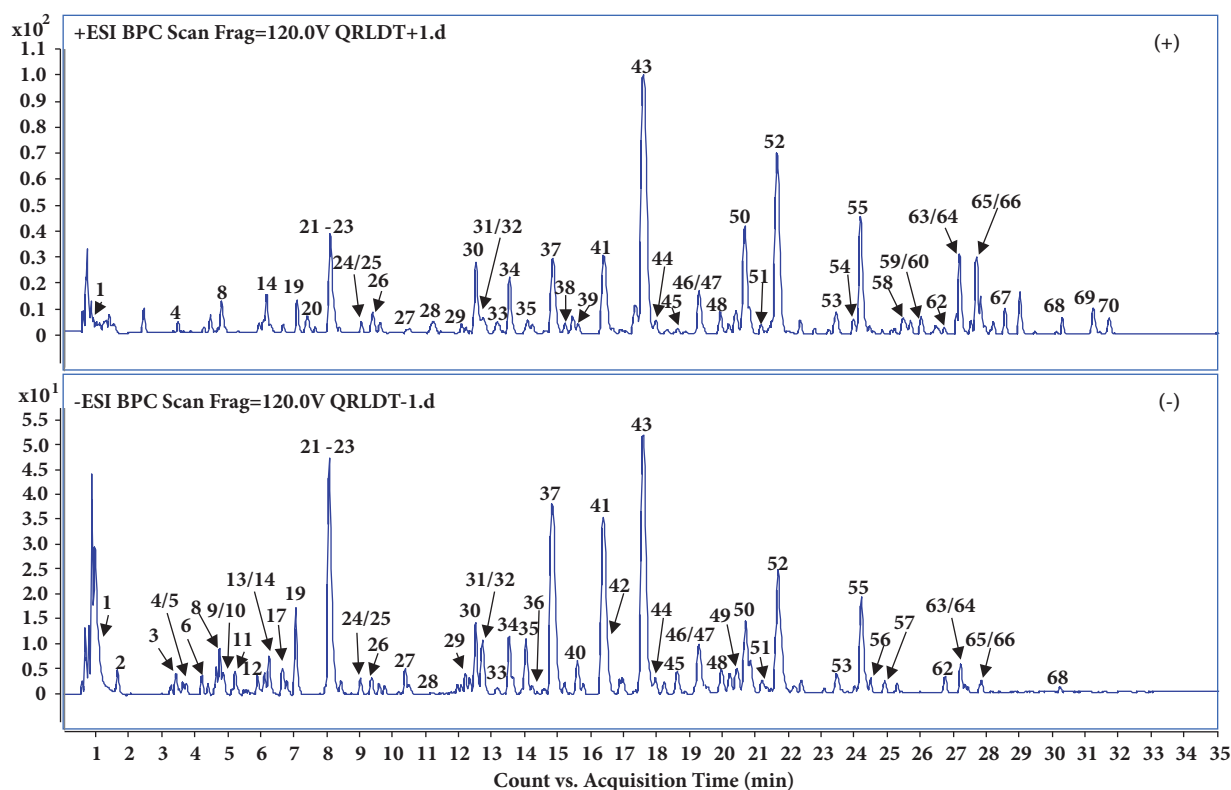


FIGURE 2: Representative base peak chromatogram (BPC) of QRLDD in the positive and negative ions mode, respectively. See Table 1 for the peak numbers, and see Section 2.3 *Chromatography and MS conditions* for UHPLC-QTOF-MS conditions.

chlorogenic acid, caffeic acid, syringin, geniposide, (-)-epicatechin, rutin, kaempferol, hesperidin, neohesperidin, baicalin, quercetin, baicalein, aloe-emodin, rhein, wogonin, emodin, dehydrocostuslactone, chrysofanol, and physcion by direct comparison of their retention time and MS Spectra with reference compounds, respectively. For the compounds without chemical standards, the molecular formula was established by high-accurate quasi-molecular ion such as $[M-H]^-$, $[2M-H]^-$, $[M+Cl]^-$, $[M+HCOO]^-$, $[M+H]^+$ and $[M+Na]^+$ within a mass error of 10.0 ppm, fractional isotope abundance, and their fragmentation patterns with related literatures. Information regarding the 72 constituents, such as t_R (min), identification, formula, negative ion (m/z), positive ion (m/z), and source, is offered in Table 1, and the exact identification of each group of components is outlined in Table 1 and Figure 2.

3.1.1. Identification of Flavones. A total of 33 flavones and their glycosides were screened from *Scutellariae Radix*, *Gardeniae Fructus*, *Aurantii Fructus*, and *Lysimachiae Herba* of QRLDD, with 9 of them unambiguously elucidated and the other tentatively identified. With respect to the glycosides, their MS spectra afforded the aglycone product due to the cleavage at the glycosidic linkage, with 146 Da, 162 Da, and 176 Da as the characteristic neutral loss of rhamnosyl, glucosyl, and glucuronic acid residues, respectively. MS² spectra with high energy showed characteristic $^{1,3}A^-$ and $^{1,3}B^-$ ions origin from a retro-Diels-Alder (RDA) cleavage of C ring as well as

losses of CH_3 (15 Da), CO (28 Da), H_2O (18 Da), CO_2 (44 Da), and/or combination of the fragments above-mentioned.

(1) Dihydroflavones. A total of seven dihydroflavones were identified from QRLD samples, with peaks 35, 40, and 41 definitely elucidated and the others tentatively assigned. Peaks 40 and 41 were accurately identified as hesperidin and neohesperidin by compared with their respective references. Corresponding to the previous paper [19], high-accurate quasi-molecular ions of peak 41 were obtained in negative ion mode at m/z 609.1823, which was identified as hesperidin. The quasi-second-order precursor ions at m/z 301.0719 and 463.1240 were generated from m/z 609.1823 ($[M-H]^-$), suggesting continuous losses of glucosyl (162 Da) and rhamnosyl (146 Da). The most dominate ions at m/z 151 and m/z 149 were yielded from m/z 301.0719 owing to RDA reaction by breaking two C-C bonds of C-ring (Figure 3(a)). Similarly, Peak 35 exhibited the $[M-H]^-$ ion at m/z 579.1709 ($C_{27}H_{32}O_{14}$, retention time 14.09 min) as well as the ions at m/z 151 and m/z 119 yielded from m/z 271.0621 $[M-H-glc-rha]^-$ through RDA reaction. The latter was 30 Da ($-CH_2O$) lower than that of Peak 41. Therefore, it was identified as narirutin, a methoxy-substituted derivative at C-6 position, according to the above information and literature [20]. Correspondingly, peaks 31, 32, 37, and 53 were tentatively assigned as carthamidin, neoericiotrin, naringin, and hesperetin based on in-house library for QRLDD and further fragmentation patterns mentioned above.

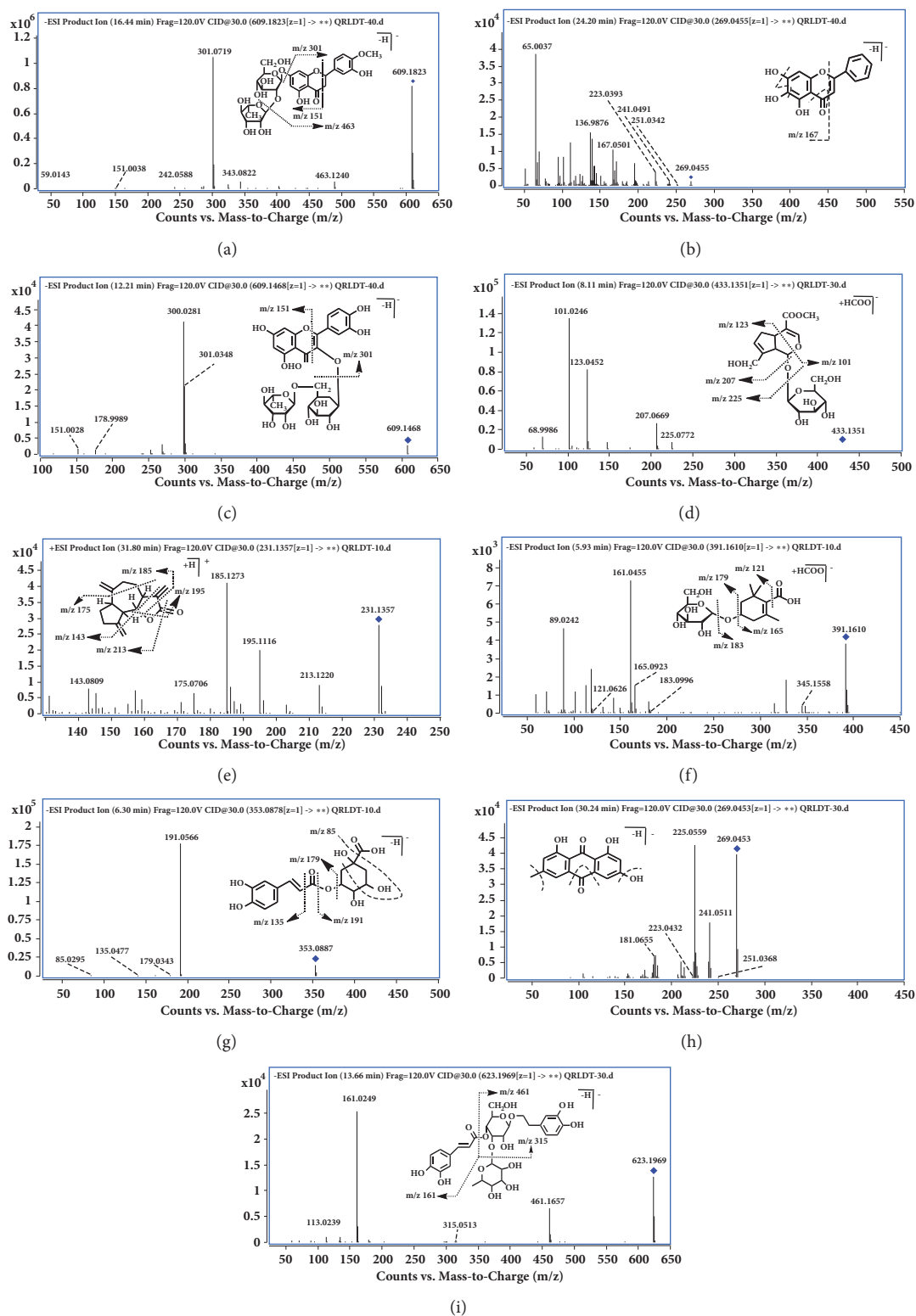


FIGURE 3: QTOF-ESI-MS/MS spectra and proposed fragmentation pathways of neohesperidin (a), baicalein (b), rutin (c), geniposide (d), jasminoside B (f), chlorogenic acid (g), emodin (h), and acteoside (i) in negative ion mode and dehydrocostuslactone (e) in positive ion mode.

(2) *Flavones and Their Glycosides*. Twenty-five flavones and their glycosides were unambiguously or tentatively identified. Peak 55, a representative major constituent in QRLDD, was taken as an example. It displayed quasi-molecular ion $[M-H]^-$ at m/z 269.0455 and was unequivocally identified as baicalein in comparison with an authentic standard. In the MS/MS spectrum, characteristic fragment ions m/z 251, 241, and 223 were formed by successive losses of H_2O (18 Da) and CO (28 Da), while the most dominant ions at m/z 167.0501 were yielded through RDA reaction (Figure 3(b)).

Similarly, peak 43 (definitely identified as baicalin) displayed a quasi-molecular ion $[M-H]^-$ at m/z 445.0773 and aglycone ion (m/z 269) that resulted from the loss of a glucuronic acid (176 Da) by easy cleavage of glycosidic bond. With similar fragmentation patterns as baicalein, fragment ions at m/z 251, 241, 223, and 167 were also detected. Thus, the fragmentation features of *O*-linked glycosyls and fragment ions of aglycones were applied in the characterization of the remaining flavones glycosides

In addition, cyclization reaction was also observed in part of flavones and their glycosides.

Peak 29 was selected as the example for the stepwise elucidation of this appearance. It was identified as rutin by comparing with authentic standard, which exhibited quasi-molecular ion $[M-H]^-$ at m/z 609.1466. Its MS^2 spectra gave the ions at m/z 463.0896 and m/z 301.0346, indicating the successive loss of rhamnose and rutinoside, while, except for similar skeleton with baicalein (Peak 55), m/z 178 and m/z 151 generated by cyclization reaction after RDA reaction in the C ring were also observed in the MS/MS spectrum (Figure 3(c)). Analogically, the other compounds were tentatively assigned following this fragmentation pathway and related literatures.

3.1.2. Identification of Terpenes. Seventeen terpenoids, including nine iridoids and their glycosides, three sesquiterpenoids, three diterpenes, and two monoterpenes, were screened from QRLDD. Among them, peaks 21 and 70 were unambiguously identified as geniposide and dehydrocostuslactone by comparison with reference standards.

(1) *Iridoids and Their Glycosides*. Peak 21 exhibited $[M+HCOO]^-$ ion at m/z 433.1351 ($C_{17}H_{24}O_{10}$, retention time 8.11 min) in negative ion mode. It produced characterized MS^2 fragment ions at m/z 225, m/z 207, m/z 123, and m/z 101 owing to the glycosidic linkage, further dehydration at C_1 and C_9 positions, and RDA reaction between C_1-O_2 and C_4-C_5 , respectively (Figure 3(d)). Similarly, peak 9 with a $[M+HCOO]^-$ ion at m/z 449.1300 ($C_{17}H_{24}O_{11}$, retention time 3.58 min) was 16 Da (+O) higher than quasi-molecular ion of peak 21. It also produced a desugarization ion at m/z 225.0772. Its predominant fragment ions at m/z 139 and m/z 101 were obtained owing to the RDA reaction. The former was 16 Da (+O) higher than that of Peak 21. Thus, this compound was tentatively assigned as scandoside methyl ester according to publications [21]. Analogously, the remaining compounds were tentatively identified by comparison of their retention behavior and MS/MS spectrum with the literature date [21, 22].

(2) *Sesquiterpenoids*. Two distinct peaks 69 and 70 with $[M+H]^+$ ions at m/z 233.1535 and 231.1357 were observed in positive ion mode, respectively. Their most probable molecular formulas were inferred to be $C_{15}H_{20}O_2$ and $C_{15}H_{18}O_2$ according to exact molecular weight. Compound 70 was identified as dehydrocostuslactone by comparison with its standard. Its tandem mass spectra and possible fragmentation pathway was illustrated in Figure 3(e). It showed the protonated ion at m/z 231.1357. The fragment ions at m/z 213, 185, 157, 195, and 175 were the characteristic behavior owing to successive neutral losses of H_2O , CH_2O_2 , $C_3H_6O_2$, H_2O_4 , and C_4H_8 , respectively [23]. Compound 69 was accordingly identified as costus lactone in a similar way. In addition, Peak 59 from *Scutellariae radix* was observed in negative ion mode and identified as dikamaliartanes A on the basis of MS data and related literature [22].

(3) *Diterpenes and Monoterpenoid Glycoside*. Three diterpenes were detected in QRLDD in negative ion mode. Peak 48 gave an $[M-H]^-$ ion at m/z 813.3186 and showed fragment ions at m/z 651, 489, and 327 by simultaneous losses of glucosyl groups (162 Da), which was deduced to crocin-2 based on the exact molecular formulae matching, fragmentation, and literature date [22]. Peak 44 and 56 exhibited the same $[M-H]^-$ ion at m/z 975.3715 ($C_{44}H_{64}O_{24}$, retention times 18.03 and 24.49 min), which was 162 Da ($+C_6H_{10}O_5$) higher than that of peak 48. They also showed the same fragments ions with Peak 48. By matching the constructed compound library, they were deduced to crocin-1 and crocin-4, a pair of cis-trans isomer originated from *Gardeniae Fructus*. In addition, as the polarity of cis-diterpenes was larger than that of trans-diterpenes, peaks 44 and 56 were identified as crocin-1 and crocin-4, respectively [22, 24].

Two monoterpenoids from *Gardeniae Fructus* were tentatively identified and their cleavage pathway is similar to that of iridoid glycosides with slightly differences. The losses of glycosides (162 Da), CO_2 (44 Da), and H_2O (18 Da) were the characteristic fragmentations in their MS^2 spectra [22, 25]. Peak 12 was selected as the example for the stepwise elucidation of the molecular structure. It yielded the ions at m/z 183.0996 and m/z 165.0923, which corresponded to successive losses of a glycoside and H_2O , respectively. The former further produced a fragment ion at m/z 121.0626 $[M-H-glc-CO_2]^-$. Consequently, Peak 12 was reasonably deduced to be jasminoside B according to aforementioned fragmental information and reference data (Figure 3(f)) [22]. Peak 39 was tentatively assigned as jasminoside S/H/I following this fragmentation pathway; however, it needed to be confirmed by the reference standards.

3.1.3. Identification of Phenolic Acids. Nine phenolic acids, originated from *Scutellariae Radix*, *Lysimachiae Herba*, and *Gardeniae Fructus*, were detected as minority of components in QRLDD. The negative ion mode was much more suitable for their analysis. Peaks 2, 3, 10, 15, and 17 were unambiguously identified as gallic acid, protocatechuic acid, 4-hydroxybenzoic acid, chlorogenic acid, and caffeic acid by comparison with authentic references. Peaks 16 and 24 were tentatively identified as darendoside A and p-coumaric

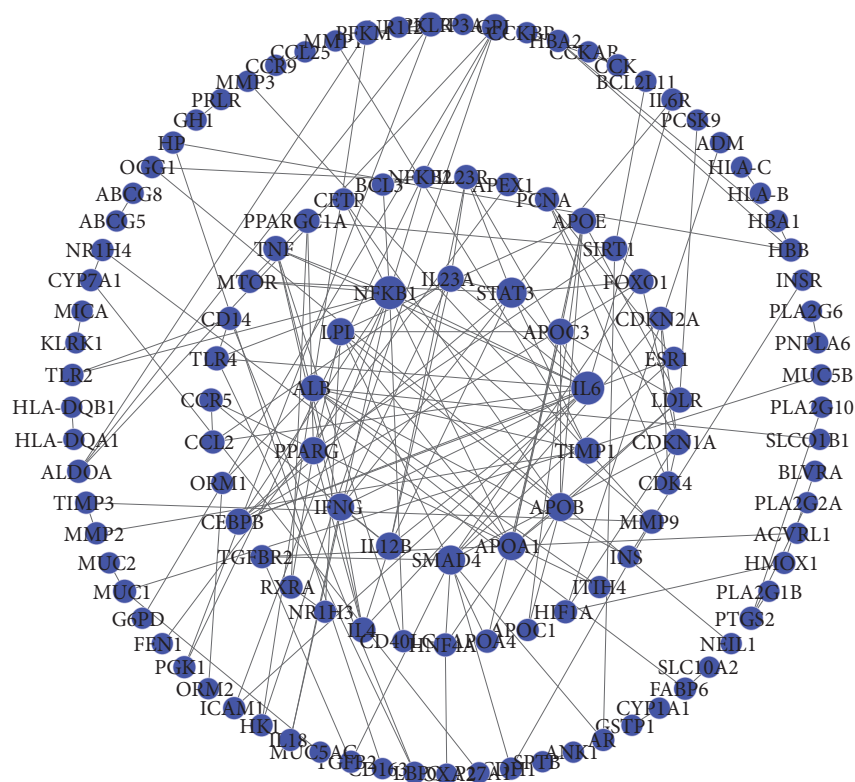


FIGURE 4: Cholelithiasis-related targets PPI network (confidence score >0.95).

acid on the basis of the exact molecular formulae matching, fragmentation, and the literature date [22, 26]. Take chlorogenic acid (Peak 15) for example. Its MS chromatograms exhibited a quasi-molecular ion at m/z 353.0890 $[M-H]^-$ as well as two diagnostic fragment ions at m/z 191.0563 (loss of a caffeoyl group, 162 Da) and 179.0343 (loss of a quinic acid, 174 Da). Another fragment ion at m/z 135.0477 was formed by the neutral losses of CO_2 (44 Da) via the break of ester bond in caffeic acid. In addition, m/z 85.0295 formed via the breaks of C_3-C_4 and C_5-C_6 as well as successive neutral loss of CO_2 was also observed (Figure 3(g)) [22]. Additionally, peaks 7 and 18 exhibited the $[M-H]^-$ ions at m/z 353.0882 and 353.0883 with molecular formula speculated as $C_{16}H_{18}O_9$, the fragment ions at m/z 191.0227 and 179.0357 were the same as chlorogenic acid (15), suggesting that they should be isomers of chlorogenic acid. Tao et al. reported that three isomeric neochlorogenic acid, chlorogenic acid, and cryptochlorogenic acid were contained in *Gardeniae Fructus* [27]. Moreover, the retention time for chlorogenic acid was later and earlier than that of neochlorogenic acid and cryptochlorogenic acid in a similar UHPLC system, respectively [28]. Therefore, peaks 7 and 18 were tentatively identified as neochlorogenic acid and cryptochlorogenic acid, respectively.

3.1.4. Identification of Anthraquinones. Five anthraquinones were unambiguously identified by comparison with authentic references, which were more suitable for the analysis in negative ion mode. Successive or simultaneous neutral losses

of H_2O , CO , O , and CH_3 were the characteristic behavior of this type of compounds. Peak 68 ($t_R = 30.24$ min) was selected as an example, which displayed the $[M-H]^-$ ion at m/z 269.0453. The yield ion at m/z 241.0511 was formed by direct loss of the CO , followed by the loss of O , and gave the ion at m/z 225.0559. The fragment ion of m/z 181, 251, and 223 was corresponded to the losses of CO_2 , H_2O , and CO , respectively (Figure 3(h)). Similarly, aloemodin, rhein, chrysophanol, and physcion were elucidated [24].

3.1.5. Identification of Phenethylalcohol Glycosides. Three phenethylalcohol glycosides were tentatively identified due to the absence of reference standards, which were from *Scutellariae Radix* and *Lysimachiae Herba*. Caffeic acid, hydroxytyrosol, and glycosyls were the basic groups of this type of compounds. Peak 34 was selected as the example for the stepwise elucidation. Peak 34 with the quasi-molecular ion m/z 623.1969 and product ions at m/z 461.1657, m/z 315.1010, and m/z 161.0249 were detected in the MS/MS spectrum. The product ions were generated from m/z 623.1981 by loss of a caffeoyl group (162 Da), m/z 461.1675 by loss of rhamnosyl residue (146 Da), and m/z 179.0353 by elimination of H_2O (18 Da), respectively (Figure 3(i)). It was identified as acteoside in consistent with the fragment information of literature [29]. Analogously, the remaining peaks 46 and 50 were tentatively identified as isomers cistanoside D and cistanoside C following above fragmentation pathway and polarity feature [29].

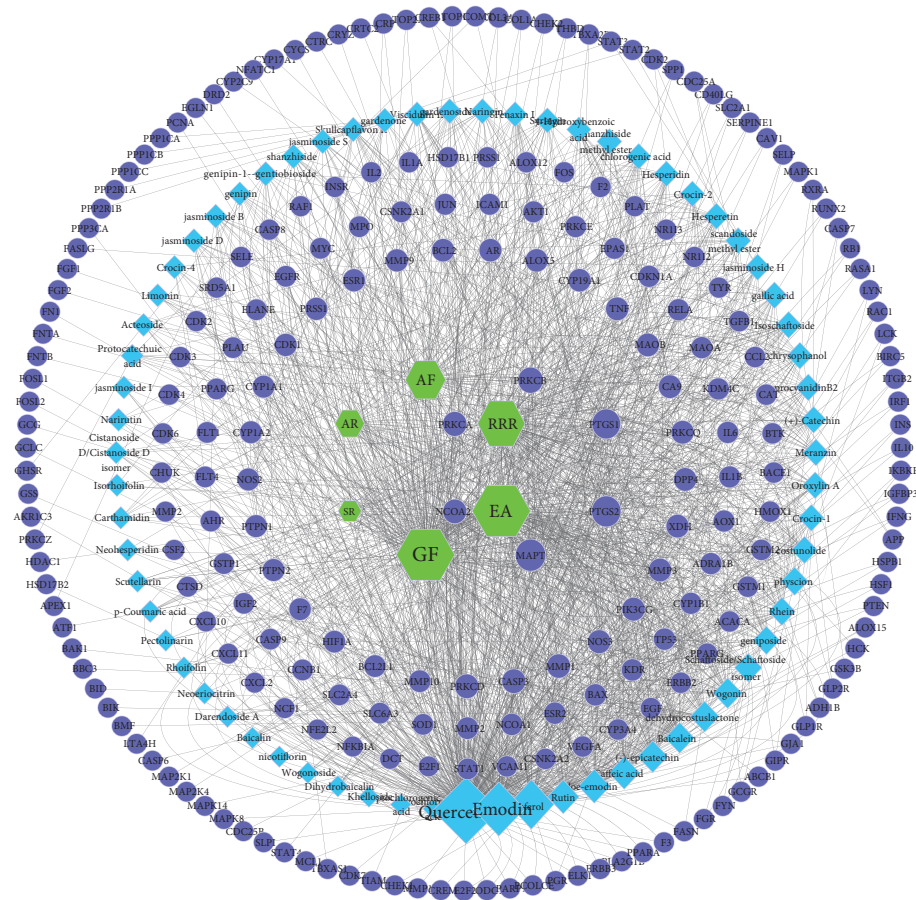


FIGURE 5: Herb-compound-compound target network of QRLDD (blue circle represents compound targets, cyan diamond represents for compound, and green hexagon represents herb; node size represents the degree).

3.1.6. *Other Types of Miscellaneous Compounds.* Other compounds (peaks 1, 11, 20, 58, and 62) were tentatively assigned as galloyl glucose, procyanidin B₂, syringin, meranzin, and limonin, respectively, on the basis of the exact molecular formulae matching, fragmentation information as well as the literature data [30–32] but still need to be further confirmed by reference standard.

3.2. Target Identification and Network Analysis

3.2.1. *Cholelithiasis-Related Targets Network Analysis.* The relationship among 410 disease genes from PPI was extracted by STRING. And a gene-gene interaction network was accordingly constructed. 122 nodes and 173 edges were involved in this network (Figure 4). Among them, the nodes located at the central part (IL6, NFKB1 and STAT3) connected by more edges have higher degree, such as 13 in IL6, 13 in NFKB1, and 10 in STAT3. It implies that these genes may be the important targets in the formation and development of cholelithiasis.

3.2.2. *Herb-Compound-Compound Targets Network Analysis.* The relationship among 432 compound targets from PPI were constructed and analyzed by STRING. Compound targets of

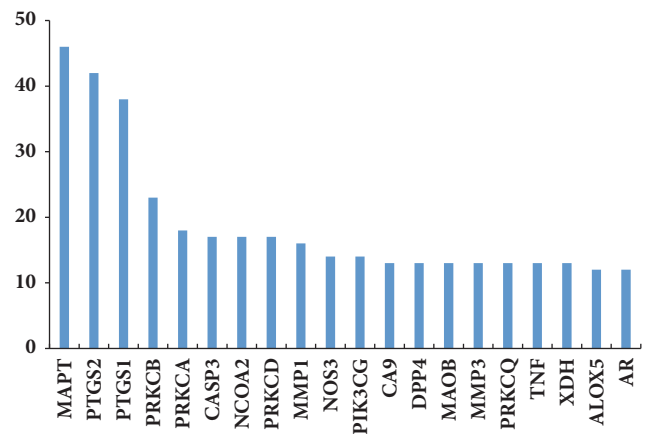


FIGURE 6: Degree of top 20 compound targets.

PPI with high confidence score (>0.95) were screened. And herb-compound-compound targets network constructed by cytoscape was shown in Figure 5, which comprises 313 nodes (6 herb nodes, 67 compound nodes, and 240 compound target nodes) and 1937 edges. From this network, we can conclude that Gardeniae Fructus, lysimachiae Herba, and

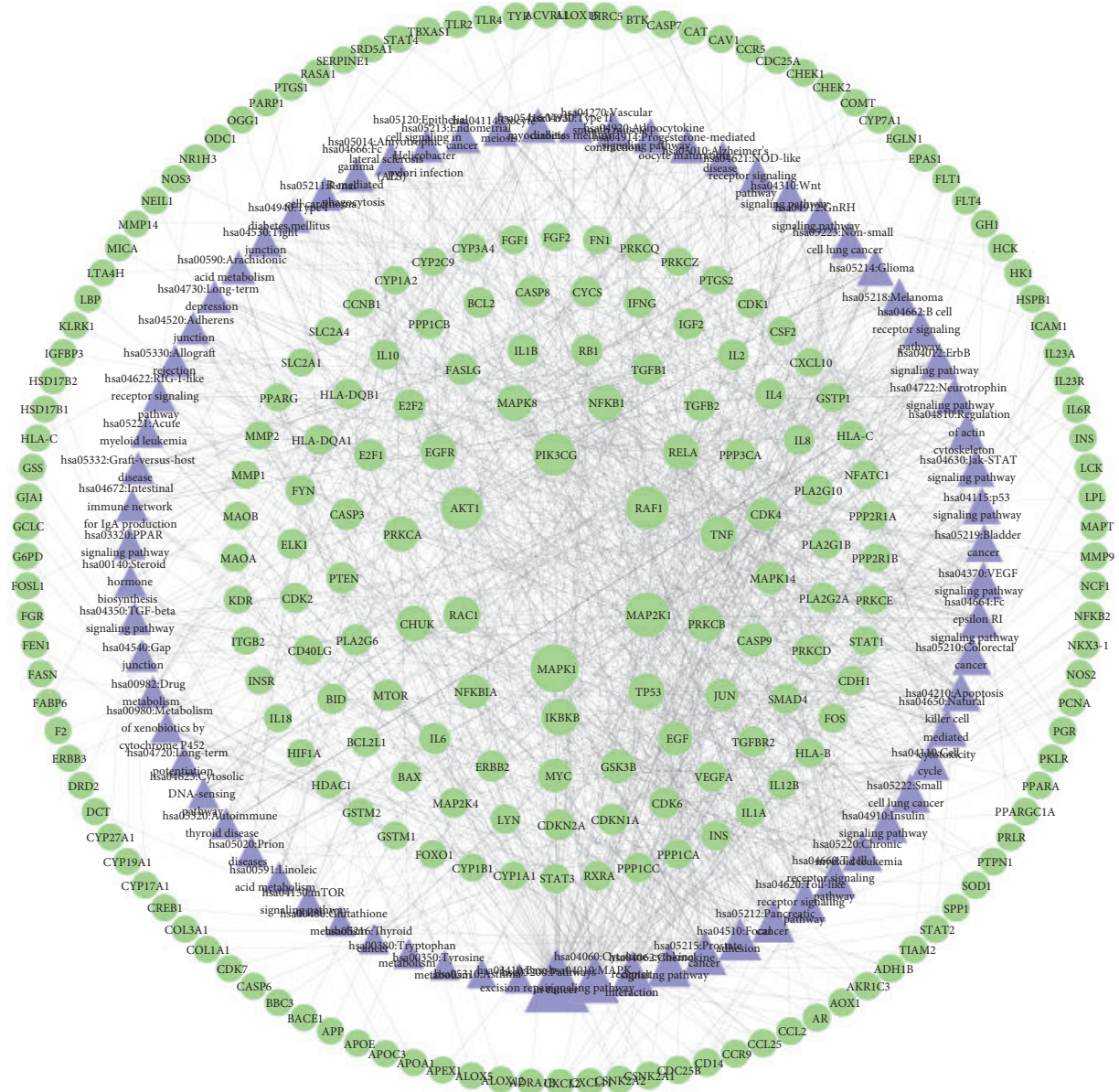


FIGURE 7: Illustration of relations among chemical constituent targets and involved pathways of QRLDD (green circle represents compound target, blue triangle represents pathway, green hexagon represents herb, and purple hexagon represents pathway. Node size represents the degree).

Scutellariae Radix may be the main herbs in treating disease due to their higher degree. According to the frequency statistics of 77 Chinese medicine cases on gallstones, *Lysimachiae Herba*, *Scutellariae Radix*, *Aurantii Fructus*, and *Aucklandiae Radix* were used for 55, 47, 21, and 12 times, respectively [33]. We can also find that many compounds acting on the same target and multiple targets contacted by the same compound. For example, MAPT is the targets of aloemodin, geniposide, gallic acid, and other chemical components. Quercetin simultaneously acts on IL10, MAPK1, HSF1, among many other targets. However, some can be regulated by only one compound, such as CA9, which is simply controlled by Khelloside. The degree of top 20 targets was listed in Figure 6.

The result indicated that compounds from QRLDD may act on these targets systematically and play an important pharmacological role in treating cholelithiasis, which is in line with herbal formulae's feature of multicomponent and multi-target. The potential mechanism can be elucidated by this network.

3.2.3. Pathway of QRLDD-Disease Network. In order to better understand the mechanism of QRLDD on cholelithiasis, 71 related pathways ($P < 0.5$) were obtained by inputting all targets into DAVID; the details are described in Supplementary Table S3. As shown in Figure 7, Pathway in cancer (hsa05200) is ranked first, which has 72 genes involved; among them, PTGS2, TP53, and IL6 have a higher degree. The

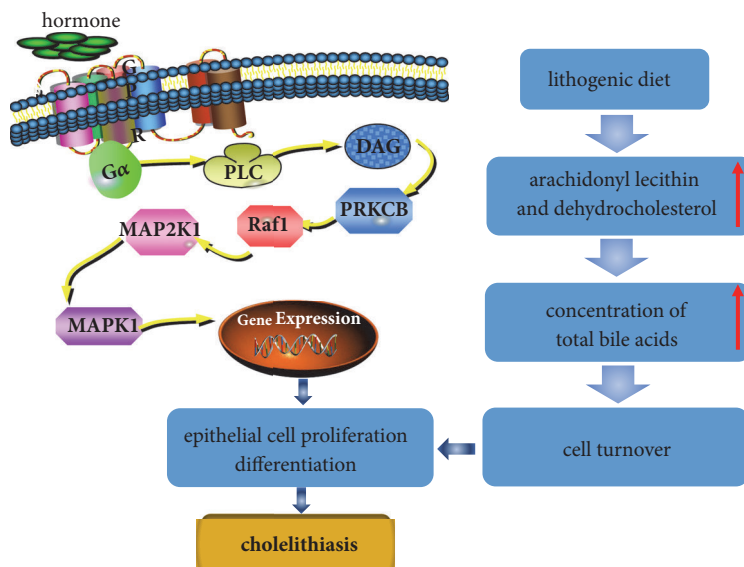


FIGURE 8: Mechanism of key targets screened by network in the formation of cholelithiasis.

result is consistent with clinical data, which confirmed the close relationship between gallstones and gallbladder cancer [34]. Within the screened genes, EGFR was selected for example, whose expression is associated with proliferation, differentiation, lymphatic metastasis, and other processes of gallbladder carcinoma [35]. Therefore, the analysis of pathways in cancer will help to understand the pathogenesis of gallbladder carcinoma caused by gallstones and provide basis for the future study.

In addition, there were 41, 35, and 31 pathways associated with MAPK1, MAP2K1, and RAF1, among which, MAPK signaling pathway (hsa04010), chemokine signaling pathway (hsa04062), and Focal adhesion (hsa04510) were the most closely related ones. KEGG data visualization made it obvious that the PRKCB downstream target proteins RAF1, MAP2K1 and MAPK1 are key connection points between the MAPK signaling pathway, chemokine signaling pathway and focal adhesion. According to previous study, lithogenic diet is closely related to the development of cholelithiasis, which tends to alter the components in bile with increasing substances such as arachidonyl lecithin and dehydrocholesterol. As an adaptive response to the environment, cell turnover will be emerged [36]. In the development of gallstone formation, mitotic index is shown to increase rapidly at prelithiasic phase [37]. In addition, the condition of gallbladder and bile duct abnormalities has been shown to accelerate the cell turnover and increase cellular proliferating activity [38]. In our present research, regulation of PRKCB/RAF1/MAP2K1/MAPK1 can affect cell proliferation and differentiation (Figure 8). These changes may provide a new perspective for the treatment of cholelithiasis.

Above findings provide a direct connection between metabolic syndrome and cholesterol gallstone. Whether their expression is involved in the curative effect of QRLDD acting on cholelithiasis will be validated in the subsequent research.

4. Conclusions

Chinese medicine plays an important role in preventing and treating cholelithiasis. In our study, the chemical profile of Qingre Lidan Decoction was mapped for the first time by UHPLC-QTOF-MS, and 72 ingredients origin from six herbs were attributed. The “multicomponent-multitarget-multipath” mechanism of QRLDD was further explored based on network pharmacology platform in view of the identified ingredient. Our study found that multiple ingredients in QRLDD can exert a combined effect for the same target. Several important targets (EGFR and MAPK1) and pathways (pathways in cancer and MAPK signaling pathway) were predicted to be an important role in the mechanism of QRLDD. The present study not only provide experimental and theoretical basis for the further development and application of QRLDD, but also make beneficial exploration in investigating the molecular synergy of Traditional Chinese Formula.

Data Availability

The data used to support the findings of this study are available from the corresponding author upon request.

Conflicts of Interest

All authors have no financial or scientific conflicts of interest in regard to the research described in this manuscript.

Acknowledgments

This work was financially supported by grants from Key Project Supported by the Clinical Ability Construction of

Liaoning Province (no. LNCCC-A03-2015), Dalian Municipal Medical Research Foundation (no. 17Z2001), and Natural Science Foundation of Institute of Integrative Medicine, Dalian Medical University (no. ICIM2017003).

Supplementary Materials

Table S1: therapeutic targets of cholelithiasis; Table S2: compound targets for QRLDD; Table S3: pathway enrichment analysis of QRLDD-Disease targets network. (*Supplementary Materials*)

References

- [1] F. Cheung, "TCM: made in China," *Nature*, vol. 480, no. 7378, pp. S82–S83, 2011.
- [2] C. J. Wang, X. M. Ma, Z. F. Wang, and et al., "Clinical Observation on Qingre Lidan Decoction in Treatment of Chronic Cholecystitis of Hepatobiliary Damp-Heat Type," *Journal of Liaoning University of Traditional Chinese Medicine*, vol. 16, pp. 183–186, 2014.
- [3] X. L. Zhu, "Clinical observation on effect of *Corydalis adunca* Maxim combined with modified Qingre Lidan Panshi decoction in the treatment of cholelithiasis," *Asia-Pacific Traditional Medicine*, vol. 14, no. 2, pp. 195–196, 2018.
- [4] J. S. Tian, Y. F. Lin, Y. Gong, and et al., "Study of the prevention of recurrence of common duct stones after ERCP/EST by Jijian Huashi Lidan Decoction," *Chinese Archives of Traditional Chinese Medicine*, vol. 31, no. 1, pp. 204–205, 2013.
- [5] K. Goh, M. E. Cusick, D. Valle, B. Childs, M. Vidal, and A. Barabási, "The human disease network," *Proceedings of the National Academy of Sciences of the United States of America*, vol. 104, no. 21, pp. 8685–8690, 2007.
- [6] A. Barabási and Z. N. Oltvai, "Network biology: understanding the cell's functional organization," *Nature Reviews Genetics*, vol. 5, no. 2, pp. 101–113, 2004.
- [7] A. L. Hopkins, "Network pharmacology: the next paradigm in drug discovery," *Nature Chemical Biology*, vol. 4, no. 11, pp. 682–690, 2008.
- [8] Y. H. Li, C. Y. Yu, X. X. Li, and et al., "Therapeutic target database update 2018: enriched resource for facilitating bench-to-clinic research of targeted therapeutics," *Nucleic Acids Research*, vol. 46, no. 1, pp. 1121–1127, 2018.
- [9] A. Hamosh, A. F. Scott, J. S. Amberger, C. A. Bocchini, and V. A. McKusick, "Online Mendelian Inheritance in Man (OMIM), a knowledgebase of human genes and genetic disorders," *Nucleic Acids Research*, vol. 33, pp. D514–D517, 2005.
- [10] J. M. Barbarino, M. Whirl-Carrillo, R. B. Altman, and T. E. Klein, "PharmGKB: A worldwide resource for pharmacogenomic information," *Wiley Interdisciplinary Reviews Systems Biology & Medicine*, vol. 10, no. 4, p. 1414, 2018.
- [11] D. S. Wishart, Y. D. Feunang, A. C. Guo et al., "DrugBank 5.0: A major update to the DrugBank database for 2018," *Nucleic Acids Research*, vol. 46, no. 1, pp. D1074–D1082, 2018.
- [12] K. G. Becker, K. C. Barnes, T. J. Bright, and S. A. Wang, "The genetic association database," *Nature Genetics*, vol. 36, no. 5, pp. 431–432, 2004.
- [13] J. Piñero, Á. Bravo, N. Queralt-Rosinach et al., "DisGeNET: A comprehensive platform integrating information on human disease-associated genes and variants," *Nucleic Acids Research*, vol. 45, no. D1, pp. D833–D839, 2017.
- [14] T. UniProt Consortium, "UniProt: the universal protein knowledgebase," *Nucleic Acids Research*, vol. 46, no. 5, p. 2699, 2018.
- [15] X. X. Li, J. Yin, J. Tang et al., "Determining the Balance Between Drug Efficacy and Safety by the Network and Biological System Profile of Its Therapeutic Target," *Frontiers in Pharmacology*, vol. 9, p. 1245, 2018.
- [16] B. Demchak, T. Hull, M. Reich et al., "Cytoscape: The network visualization tool for GenomeSpace workflows," *F1000Research*, vol. 3, article 151, 2014.
- [17] S. Li and B. Zhang, "Traditional Chinese medicine network pharmacology: theory, methodology and application," *Chinese Journal of Natural Medicines*, vol. 11, no. 2, pp. 110–120, 2013.
- [18] D. W. Huang, B. T. Sherman, and R. A. Lempicki, "Systematic and integrative analysis of large gene lists using DAVID bioinformatics resources," *Nature Protocols*, vol. 4, no. 1, pp. 44–57, 2009.
- [19] N. Fabre, I. Rustan, E. De Hoffmann, and J. Quetin-Leclercq, "Determination of flavone, flavonol, and flavanone aglycones by negative ion liquid chromatography electrospray ion trap mass spectrometry," *Journal of The American Society for Mass Spectrometry*, vol. 12, no. 6, pp. 707–715, 2001.
- [20] J. Zhang, W. Gao, Z. Liu, Z. Zhang, and C. Liu, "Systematic analysis of main constituents in rat biological samples after oral administration of the methanol extract of fructus aurantii by HPLC-ESI-MS/MS," *Iranian Journal of Pharmaceutical Research*, vol. 13, no. 2, pp. 493–503, 2014.
- [21] Z. Fu, R. Xue, Z. Li et al., "Fragmentation patterns study of iridoid glycosides in Fructus Gardeniae by HPLC-Q/TOF-MS/MS," *Biomedical Chromatography*, vol. 28, no. 12, pp. 1795–1807, 2014.
- [22] L. Wang, S. Liu, X. Zhang, J. Xing, Z. Liu, and F. Song, "A strategy for identification and structural characterization of compounds from Gardenia jasminoides by integrating macroporous resin column chromatography and liquid chromatography-tandem mass spectrometry combined with ion-mobility spectrometry," *Journal of Chromatography A*, vol. 1452, pp. 47–57, 2016.
- [23] J. Zhang, X. Hu, W. Gao et al., "Pharmacokinetic study on costunolide and dehydrocostuslactone after oral administration of traditional medicine Aucklandia lappa Decne. by LC/MS/MS," *Journal of Ethnopharmacology*, vol. 151, no. 1, pp. 191–197, 2014.
- [24] G.-D. Zheng, K. Li, Y.-S. Li, and E.-H. Liu, "Fast profiling of chemical constituents in Yiqing Capsule by ultra-performance liquid chromatography coupled to electrospray ionization tandem mass spectrometry," *Journal of Separation Science*, vol. 35, no. 1, pp. 174–183, 2012.
- [25] X. Zhao, J. Wei, and M. Yang, "Simultaneous Analysis of Iridoid Glycosides and Anthraquinones in Morinda officinalis Using UPLC-QqQ-MS/MS and UPLC-Q/TOF-MSE," *Molecules*, vol. 23, no. 5, p. 1070, 2018.
- [26] W. Liu, H. Wang, B. Zhu et al., "An activity-integrated strategy of the identification, screening and determination of potential neuraminidase inhibitors from Radix Scutellariae," *PLoS ONE*, vol. 12, no. 5, p. e0175751, 2017.
- [27] Y. Wang, J. Wen, W. Zheng et al., "Simultaneous determination of neochlorogenic acid, chlorogenic acid, cryptochlorogenic acid and geniposide in rat plasma by UPLC-MS/MS and its application to a pharmacokinetic study after administration of Reduning injection," *Biomedical Chromatography*, vol. 29, no. 1, pp. 68–74, 2015.
- [28] L. Tao, Z. Lin, J. Chen, Y. Wu, and X. Liu, "Mid-infrared and near-infrared spectroscopy for rapid detection of Gardeniae

- Fructus by a liquid-liquid extraction process,” *Journal of Pharmaceutical and Biomedical Analysis*, vol. 145, pp. 1–9, 2017.
- [29] X. Qiao, R. Li, W. Song, and et al., “A targeted strategy to analyze untargeted mass spectral data: Rapid chemical profiling of *Scutellaria baicalensis* using ultra-high performance liquid chromatography coupled with hybrid quadrupole orbitrap mass spectrometry and key ion filtering,” *Journal of Chromatography A*, vol. 1441, pp. 83–95, 2016.
- [30] Z. Liang, T. Sham, G. Yang, L. Yi, H. Chen, and Z. Zhao, “Profiling of secondary metabolites in tissues from *Rheum palmatum* L. using laser microdissection and liquid chromatography mass spectrometry,” *Analytical and Bioanalytical Chemistry*, vol. 405, no. 12, pp. 4199–4212, 2013.
- [31] S. Wu, K. Dastmalchi, C. Long, and E. J. Kennelly, “Metabolite profiling of jaboticaba (*Myrciaria cauliflora*) and other dark-colored fruit juices,” *Journal of Agricultural and Food Chemistry*, vol. 60, no. 30, pp. 7513–7525, 2012.
- [32] X. Y. Liu, M. L. Fan, H. Y. Wang, B. Y. Yu, and J. H. Liu, “Metabolic profile and underlying improved bio-activity of *Fructus aurantii immaturus* by human intestinal bacteria,” *Food & Function*, vol. 8, no. 6, pp. 2193–2201, 2017.
- [33] S. J. Ma, W. J. Zhang, J. W. Sheng et al., “Analysis on composition principles of prescriptions for cholelithiasis by using Traditional Chinese Medicine Inheritance Support System,” *Journal of Hebei TCM and Pharmacology*, vol. 33, pp. 36–39, 2018.
- [34] C. Boutros, M. Gary, K. Baldwin, and P. Somasundar, “Gallbladder cancer: past, present and an uncertain future,” *Surgical Oncology*, vol. 21, no. 4, pp. e183–e191, 2012.
- [35] S. R. E. Pais-Costa, J. F. D. M. Farah, R. Artigiani-Neto, S. J. O. Martins, and A. Goldenberg, “Evaluation of P53, E-cadherin, Cox-2, and EGFR protein immunoexpression on prognostic of resected gallbladder carcinoma,” *Arquivos brasileiros de cirurgia digestiva : ABCD = Brazilian archives of digestive surgery*, vol. 27, no. 2, pp. 126–132, 2014.
- [36] R. Sakata, T. Aoki, T. Ueno et al., “Morphological observation on extrahepatic bile duct of golden hamsters fed a lithogenic diet: Histochemical, ultrastructural and cell kinetic studies,” *Digestion*, vol. 55, no. 4, pp. 253–259, 1994.
- [37] H. J. Chang, J. I. Suh, and S. Y. Kwon, “Gallstone formation and gallbladder mucosal changes in mice fed a lithogenic diet,” *Journal of Korean Medical Science*, vol. 14, no. 3, pp. 286–292, 1999.
- [38] M. Vakkala, J. J. Laurila, J. Saarnio et al., “Cellular turnover and expression of hypoxic-inducible factor in acute acalculous and calculous cholecystitis,” *Critical Care*, vol. 11, no. 5, p. 116, 2007.